This is an open access article published under an ACS AuthorChoice License, which permits copying and redistribution of the article or any adaptations for non-commercial purposes.

BIOCHEMISTRY
including biophysical chemistry & molecular biology

Article

pubs.acs.org/biochemistry

Conserved Amino Acid Residues of the NuoD Segment Important for Structure and Function of *Escherichia coli* NDH-1 (Complex I)

Prem Kumar Sinha,[#,†,○] Norma Castro-Guerrero,[#,†,⊥] Gaurav Patki,[†,▽] Motoaki Sato,[†,∥] Jesus Torres-Bacete,[†,◇] Subhash Sinha,[‡,□] Hideto Miyoshi,[§] Akemi Matsuno-Yagi,[†] and Takao Yagi*[,†]

[†]Deparment of Molecular and Experimental Medicine, and [‡]Department of Cell and Molecular Biology, The Scripps Research Institute, 10550 North Torrey Pines Road, MEM256, La Jolla, California 92037, United States

[§]Division of Applied Life Sciences, Graduate School of Agriculture, Kyoto University, Sakyo-ku, Kyoto 606-8502, Japan

Supporting Information

ABSTRACT: The NuoD segment (homologue of mitochondrial 49 kDa subunit) of the proton-translocating NADH:quinone oxidoreductase (complex I/NDH-1) from *Escherichia coli* is in the hydrophilic domain and bears many highly conserved amino acid residues. The three-dimensional structural model of NDH-1 suggests that the NuoD segment, together with the neighboring subunits, constitutes a putative quinone binding cavity. We used the homologous DNA recombination technique to clarify the role of selected key amino acid residues of the NuoD segment. Among them, residues Tyr273 and His224 were considered candidates for having important interactions with the quinone headgroup. Mutant Y273F retained partial activity but lost sensitivity to capsaicin-40. Mutant H224R scarcely affected the activity, suggesting that this residue may not be essential. His224 is located in a loop near the N-terminus of the NuoD segment (Gly217−Phe227) which is considered to form part of the quinone binding cavity. In contrast to the His224 mutation, mutants G217V, P218A, and G225V almost completely lost the activity. One region of this loop is positioned close to a cytosolic loop of the NuoA subunit in the membrane domain, and together they seem to be important in keeping the quinone binding cavity intact. The structural role of the longest helix in the NuoD segment located behind the quinone binding cavity was also investigated. Possible roles of other highly conserved residues of the NuoD segment are discussed.

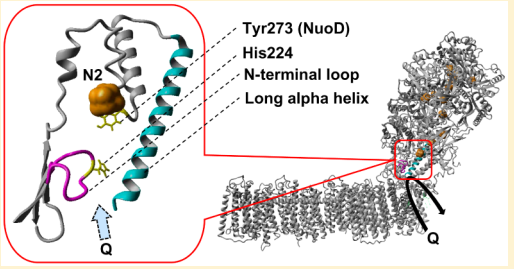

Respiratory chain complex I (NADH:ubiquinone oxidoreductase, EC 1.6.5.3) is a very large membrane protein that catalyzes the transfer of electrons from NADH to quinone (Q) linked to the translocation of protons across the membrane generating the proton-motive force required for the synthesis of ATP.[1,2] The mitochondrial enzyme is by far the largest enzyme of the respiratory chain with a molecular mass of approximately 1000 kDa and 44 different subunits described.[3,4] The bacterial enzyme (NDH-1) consists of 13−14 subunits, which are all homologues to the central core subunits of the mitochondrial enzyme with a molecular mass of approximately 550 kDa.[5−7] Complex I/NDH-1 has a characteristic L-shaped form with two clearly defined domains, a hydrophilic peripheral arm projected into the mitochondrial matrix (or bacterial cytoplasm), and a transmembrane hydrophobic arm.[1,8,9] The hydrophilic domain contains the NADH binding cavity and all known redox centers: one flavin mononucleotide and 8−9 Fe/S clusters. The peripheral arm of *Escherichia coli* NDH-1 harbors six subunits (NuoB, CD, E, F, G, and I), and all the electron transfer events before Q reduction occur in the peripheral domain.[10−12] The hydrophobic arm on the other hand is embedded in the inner mitochondrial/cytoplasmic membrane and participates in the proton translocation.[13−18]

Lately, the complex I field has seen a great advancement whereby researchers determined the crystal structures, suggesting the likely mechanisms for electron transfer and proton translocation.[8,19−22] The crystal structure suggests that the subunits NuoCD and NuoB, together with the cytoplasmic surface of NuoH, form a cavity for Q binding.[22] This region of complex I was found to be highly conserved among membrane-bound [NiFe]-hydrogenases and complex I-like oxidoreductases,[8] with subunit Nqo4 in *Thermus thermophilus* (NuoD counterpart) superimposing very well with the large subunit of the [NiFe]-hydrogenase.[11] Studies using different inhibitors of complex I have provided important structural and functional information about Q binding and reduction. The group of Miyoshi and others have shown that ND1 (*E. coli* NuoH) and 49 kDa (*E. coli* NuoD segment) are the two major subunits labeled by different inhibitors and photoaffinity probes.[23−27] The amino acid residues near terminal Fe/S cluster N2 were investigated by the group of Brandt in the strictly aerobic yeast *Yarrowia lipolytica*.[28−31] All these studies by and large point out that the inhibitors and Q bind to the interfacial region surrounded by subunits 49k (*E. coli* NuoD), PSST (*E. coli* NuoB), and ND1 (*E. coli* NuoH).[23,24,26,30,32,33] However, despite this recent progress, details of the Q binding cavity

Received: November 12, 2014
Revised: December 27, 2014
Published: December 29, 2014

 © 2014 American Chemical Society

DOI: 10.1021/bi501403t
Biochemistry 2015, 54, 753−764

including the precise residues involved in the catalysis are still unclear.

In a series of work, we have established the advantage of the chromosomal DNA manipulation technique and have shown that *E. coli* NDH-1 is ideally suited to study both membrane and peripheral domains of complex I.[13−15,18,34,35] Our method has an advantage of avoiding polar effects seen in *in trans* complementation. Moreover, there are certain merits in the bacterial system over mitochondrial complex I including the simpler structure, the absence of "assembly factors" and "accessory subunits", and no potential implications derived from protein and cofactor import that require ATP and the membrane potential.[36,37]

The NuoCD subunit is separated into two subunits in most organisms including mammals and various prokaryotes. However, the NuoCD subunit of *E. coli* NDH-1 is a single polypeptide of approximately 70 kDa, where the NuoC segment is a homologue of NuoC/Nqo5/30k subunit, while the NuoD segment is homologue of NuoD/Nqo4/49k. We previously reported a pivotal role of the third α helix in the NuoC segment in the structural stability of the NDH-1.[38]

In the present work, we investigated the NuoD segment to unveil the essential elements surrounding the Q binding cavity of NDH-1. Out of 80 highly conserved residues in the NuoD segment of *E. coli* NDH-1, we focused on 20 residues which are located near the proposed Q binding pocket.[22] The role of these residues in Q binding and architecture of NDH-1 is discussed.

MATERIALS AND METHODS

Materials. The pGEM-T Easy Vector was from Promega (Madison, WI). The site-directed mutagenesis kit (QuickchangeII XL kit) and the Herculase Enhanced DNA polymerase were obtained from Stratagene (Cedar Creek, TX). Materials for PCR product purification, gel extraction, and plasmid preparation were from Qiagen (Valencia, CA). Endonucleases were purchased from New England Biolabs (Beverly, MA). The pKO3 vector was a generous gift from Dr. George M. Church (Harvard Medical School, Boston, MA). NADH, dNADH, DB, UQ_1, and UQ_2 were purchased from Sigma-Aldrich (St. Louis, MO). *p*-Nitroblue tetrazolium was from EMD Biosciences (La Jolla, CA). Oxonol VI and ACMA were from Invitrogen (Carlsbad, CA). Capsaicin-40 and 6-azido-4-(4-iodophenetylamino) quinazoline (from hereon referred as AzQ) were from the laboratory of Dr. Hideto Miyoshi (Kyoto University, Kyoto, Japan), while squamotacin was synthesized in the laboratory of Dr. Subhash Sinha (The Scripps Research Institute).[39] Oligonucleotides were obtained from Valuegene (San Diego, CA). All other materials were reagent grade and were obtained from commercial sources.

Cloning and Mutagenesis of *E. coli nuoCD* Gene. Cloning and mutagenesis for the *E. coli nuoCD* gene were performed as described previously.[38] The amino acid residues of the NuoCD subunit starting from Met190 have been extracted on the basis of alignment to the sequences of the Nqo4/NuoD subunit and homologues from several organisms. Hereon, this part will be referred to as the NuoD segment/domain in the present work. The whole process was essentially performed according to the method described formerly by Link et al.[40] and modified by Castro-Guerrero et al.[38] In brief, an *E. coli* NuoD-KO was constructed by replacement of the *nuoD* segment gene by spectinomycin (*spc*) in the NDH-1 operon using the pKO3 system. In parallel, a DNA fragment that includes the *nuoD* segment gene together with a 1-kb upstream and 1-kb downstream DNA segments from *E. coli* DH5α was cloned in the pGEM-T Easy Vector system, generating pGEM/*nuoD*. pGEM/*nuoD* was used as a template to obtain the *nuoD* mutants. The *nuoD* mutants were then subcloned into the pKO3 vector generating the pKO3/*nuoD* mutants, which were finally used to replace the *spc* gene in *E. coli nuoD-KO* by recombination. All of the mutations were confirmed by direct DNA sequencing at various stages of cloning and mutagenesis.

Growth and Membrane Preparation of *E. coli* NuoD Segment Mutants. *E. coli* NuoD segment mutants were grown, and inverted membrane vesicles were prepared according to the method described previously.[14,35,41] Briefly, cells were grown at 37 °C overnight in 250 mL of Terrific Broth medium and then harvested by centrifugation at 5800*g* for 10 min and resuspended at 10% (w/v) in 10 mM Tris-HCl (pH 7.0), 1 mM EDTA, 1 mM dithiothreitol, 1 mM phenylmethanesulfonyl fluoride and 15% glycerol. The cell suspension was sonicated twice for 15 s and then passed twice through the French Pressure cell press (15000 p.s.i.). The cell debris was removed by centrifugation (23400*g* for 10 min), and the resultant supernatant was centrifuged again (256600*g* for 30 min). The pellet containing membrane samples was finally resuspended in the same buffer, frozen in liquid nitrogen, and stored at −80 °C until further use.

Activity Analysis. The NDH-1 mutants activity analysis was performed according to the methods described previously.[38,41] Briefly, the dNADH-$K_3Fe(CN)_6$ reductase activity was performed at 30 °C with 80 μg of protein/mL of membrane samples in 10 mM potassium phosphate (pH 7.0), 1 mM EDTA containing 10 mM KCN, and 1 mM $K_3Fe(CN)_6$. The samples were preincubated for 1 min before starting the reaction with the addition of 150 μM dNADH. The absorbance change was followed at 420 nm. $K_3Fe(CN)_6$ was replaced by 50 μM DB, 50 μM UQ_1, or 50 μM UQ_2 as electron acceptors, and the measurements were monitored at 340 nm for performing dNADH-DB, dNADH- UQ_1, or dNADH-UQ_2 reductase activity in the same buffer condition. The dNADH oxidase activity was measured in the same conditions, but without addition of KCN or DB/UQ_1/UQ_2 in the reaction buffer. Capsaicin-40, 6-azido-4-(4-iodophenetylamino) quinazoline (AzQ) and squamotacin were used for monitoring inhibition of the energy-transducing dNADH oxidase activities. The extinction coefficients used for activity calculations were ε_{340} = 6.22 $mM^{-1}\,cm^{-1}$ for deamino-NADH and ε_{420} = 1.00 $mM^{-1}\,cm^{-1}$ for $K_3Fe(CN)_6$.

Membrane potential generated by the NDH-1 mutants was monitored optically using oxonol VI as reporter.[42] The reactions were carried out at 30 °C with 0.33 mg of protein/mL of membrane samples in 50 mM MOPS (pH 7.3), 10 mM $MgCl_2$, and 50 mM KCl buffer containing 2 μM oxonol VI. The reactions were started by the addition of 200 μM dNADH, and the absorbance changes at 630−603 nm were recorded. Proton pump activity was followed using ACMA fluorescence quenching as described earlier.[41,43] 2 μM FCCP was used to dissipate membrane potential and the proton gradient across the membranes.

Immunoblotting and BN-PAGE. Antibodies against *E. coli* NDH-1 subunits NuoB, NuoCD, NuoE, NuoF, NuoG, NuoI, and NuoL were previously generated in our laboratory.[16,35,38,44] The above antibodies were used to analyze the content of the NDH-1 subunits by Western blotting. The procedures for performing BN-PAGE electrophoresis have been described

DOI: 10.1021/bi501403t
Biochemistry 2015, 54, 753−764

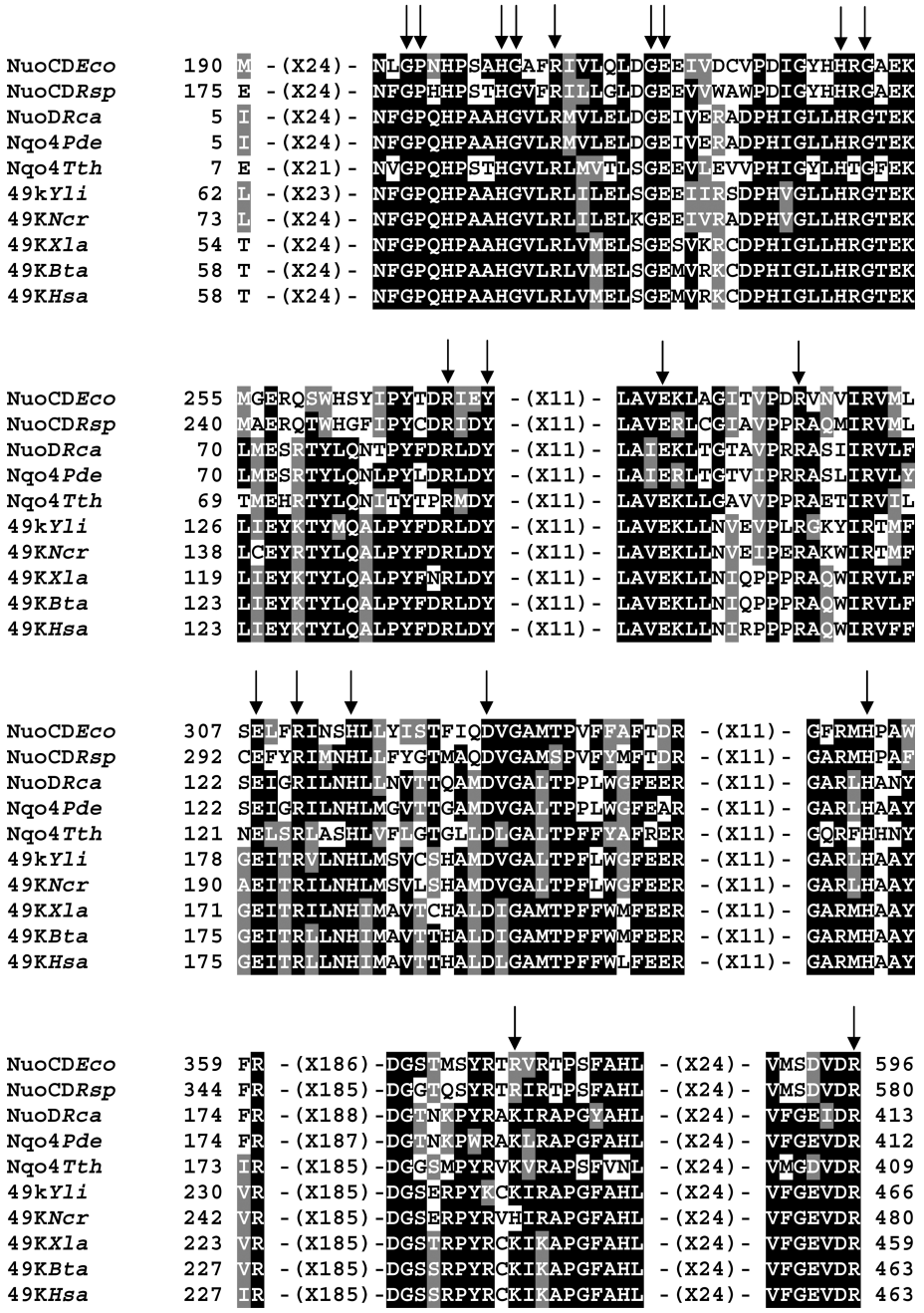

Figure 1. Partial alignment of the deduced amino acid sequences among the *E. coli* NuoD segment and its homologues from various organisms. The alignment was carried out by the ClustalW program.[62] The shading of the residues was done by the default Box-shade program based on their similarity. Amino acids mutated in this study are marked by arrows (also see Supplemental Figure 1, Supporting Information). Sequence sources and their Swiss-Prot accession numbers are NuoCD*Eco*, *E. coli* K-12 NuoCD subunit [P33599]; NuoCD*Rsp*, *Rhodobacter sphaeroides* NuoCD subunit [B9KJI1]; NuoD*Rca*, *Rhodobacter capsulatus* NuoD subunit [O07310]; Nqo4*Pde*, *Paracoccus denitrificans* Nqo4 subunit [A1B495]; Nqo4*Tth*, *T. thermophilus* HB-8 Nqo4 [Q56220]; 49K*Yli*, *Yarrowia lipolytica* 49K subunit [Q9UUU1]; 49K*Ncr*, *Neurospora crassa* 49K subunit [P22142]; 49K*Xla*, *Xenopus laevis* 49K subunit [Q32NR8]; 49K*Bta*, *Bos taurus* 49K subunit [P17694]; 49K*Hsa*, *Homo sapiens* 49K subunit [O75306].

earlier.[41] The assembly of NDH-1 was examined by NADH dehydrogenase activity staining as reported.[41]

Other Analytical Procedures. Protein concentrations were determined by using the BCA protein assay kit (Pierce) with bovine serum albumin as the standard according to the manufacturer's instructions. Any variations from the procedures and details are described in the figure legends.

Homology Modeling of *E. coli* NDH-1. The Swiss-Model web server (http://swissmodel.expasy.org) was used to obtain the 3D model for the *E. coli* NDH-1 by protein structure homology modeling.[45] The amino acid sequence of each of NuoC, NuoD, NuoB, NuoA, and NuoH was used as the target. The template structure for each target was derived from the whole structure of the *T. thermophilus* NDH-1 (4HEA)[22] as provided by the Swiss-Model template library. The coordinates of the modeled subunits thus obtained were combined and used for presentation of the structure images as well as analysis. Cluster N2 was added from the *T. thermophilus* coordinates and used for display purposes. In all figures, the amino acids were labeled using *E. coli* numbering.

DOI: 10.1021/bi501403t
Biochemistry 2015, 54, 753−764

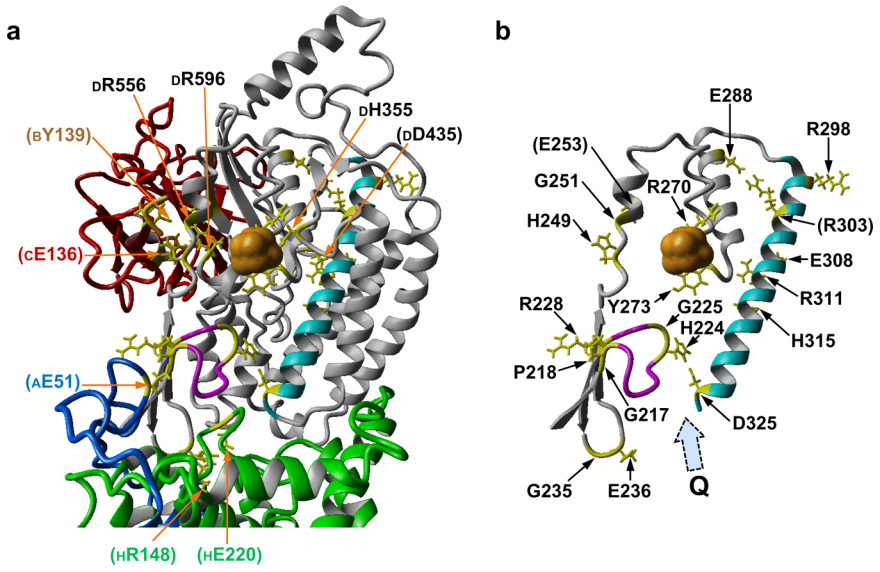

Figure 2. Structural analysis of the *E. coli* NuoD segment and the proposed Q-binding cavity. (a) Cartoon representation of the *E. coli* NuoD segment and the neighboring subunits. The 3D model for *E. coli* NuoCD, NuoH, and NuoA subunits was obtained by homology modeling based on the crystallographic data of the *T. thermophilus* enzyme[11,22] using the Swiss-Model server.[45] Visualization was done using YASARA (http://www.yasara.org). The NuoD segment, NuoC segment, NuoH, and NuoA are colored in gray, red, green, and blue, respectively. The N-terminal conserved loop and the long α helix in the NuoD segment are highlighted in magenta and light blue, respectively. Cluster N2 is illustrated in brown. The side-chains of the mutated residues are displayed in yellow. The proposed insertion angle of Q was illustrated by a dashed arrow. The locations of mutated residues in this region are shown with the residue number. Some key residues not examined in this work are also shown (in parentheses). (b) Cartoon representation of the NuoD segment depicting the region from the N-terminus to the long α helix.

RESULTS

Sequence Analysis of the NuoCD Subunit. The *E. coli* NuoCD subunit is a polypeptide of 596 amino acid residues. The amino acid residues of the NuoCD subunit from Met190 to Arg596 is referred to as the NuoD segment (or simply 'NuoD' for brevity) in the present work on the basis of alignment to the sequences of the Nqo4/NuoD subunit from several organisms. Figure 1 shows the partial alignment of the deduced amino acid sequences of subunit NuoD/Nqo4/49 kDa from diverse sources ranging from mammals to bacteria. The NuoD segment is among the most-conserved regions of NDH-1 with about 80 highly conserved amino acids.

As the reduction of Q by electrons from the terminal Fe/S cluster N2 is a key step in the catalytic mechanism, many of the residues near cluster N2 were found to be highly conserved (Figure 1; see also Supplemental Figure 1, Supporting Information). Further, the N terminal region in the bovine 49 kDa subunit (around Arg228 in *E. coli* NuoD) forms a loop that is part of the proposed Q binding cavity. On the basis of photoaffinity labeling experiments, the N-terminal region of the 49 kDa subunit (Asp74-Arg96; corresponding to Thr206-Arg228 in *E. coli* NuoD segment) was reported to interact with a complex I inhibitor, AzQ.[23] Thus, we selected several conserved residues that are present either in the immediate vicinity of cluster N2 (including Arg270, Tyr273, and His355) or in the proposed Q binding cavity including conserved residues in the loop (Gly217-Phe227), Arg228 and Asp325 (Figure 2). The mutation H95A in the 49 kDa subunit of complex I from *Y. lipolytica* was shown to be essential for ubiquinone reductase activity, though the EPR spectra for all Fe−S clusters remained unchanged.[46] Subsequently, the group of Verkhovskaya analyzed the corresponding mutation His224A in subunit NuoCD of *E. coli* complex I.[47] The ubiquinone reductase activity of this mutant in complex I was about 50% as compared to the wild-type and the EPR spectra of purified complex I from the mutant did not differ from the wild-type. Thus, in the present work, we decided to investigate an arginine mutation for the aforementioned His224 residue. Both being a basic residue, replacement of a histidine by an arginine would help in evaluating if the pK_a at this position is important for the activity or the sensitivity of inhibitors.

The NuoD segment has a prominent four α helix bundle that seems to be located in the back of the Q binding pocket and was indicated to be shifted upon reduction of cluster N2.[22] Out of these helices, we focused on the longest one, from residue Tyr273 to Asp325, which lines the cavity. Our earlier study displayed the significant role of Glu136 in the NuoC segment for the architecture of NDH-1 that is suggested to interact with Arg556 and Arg596 in the C-terminal of the NuoD segment.[38] Furthermore, the homology modeling of *E. coli* NDH-1 indicated the interaction of His249 in the NuoD segment with Tyr139 in NuoB, which is proposed to be protonated by the reduction of cluster N2.[48] Thus, to get a better understanding of the functional and structural roles of the NuoD segment, we generated a total of 36 point mutations at 20 different sites of the segment in NuoCD subunit of *E. coli* NDH-1. Multiple exchanges were also introduced at certain positions to understand how catalytic activity depends on the size and properties of a particular side chain. We have earlier mutated residues in the NuoH (ND1) subunit of the membrane domain[41] and some of them were re-examined in the present work in regard to the putative Q binding cavity.

Effects of NuoD Segment Mutation on the dNADH-$K_3Fe(CN)_6$ Reductase Activity. To measure the activities derived solely form NDH-1, we used dNADH as the substrate.[49] The dNADH-$K_3Fe(CN)_6$ reductase activity is believed to derive from the NADH dehydrogenase segment of the complex I/NDH-1 and therefore mutation in NuoD would not affect this activity if the complex I remains intact.[41]

DOI: 10.1021/bi501403t
Biochemistry 2015, 54, 753−764

Table 1. Enzymatic Activities of the Wild-Type and Various NuoD Mutants of *E. coli* NDH-1

mutant	dNADH-O_2[a]	dNADH-DB[a]	dNADH-UQ_1[a]	dNADH-UQ_2[a]	dNADH-$K_3Fe(CN)_6$[b]	ratio[c]	in *T.th*[d]	in *Y.li*[e]
WT	706 ± 47 (100%)	870 ± 55 (100%)	973 ± 44 (100%)	1508 ± 28 (100%)	1724 ± 33 (100%)	2.4		
NuoD-KO	8 ± 1 (1%)	19 ± 1 (2%)	44 ± 3 (4%)	18 ± 2 (1%)	408 ± 43 (24%)	51.0		
KO-rev	589 ± 28 (86%)	763 ± 16 (88%)	746 ± 18 (77%)	1463 ± 34 (97%)	1779 ± 19 (103%)	3.0		
G217V	10 ± 1 (1%)	56 ± 5 (6%)	41 ± 1 (4%)	32 ± 2 (2%)	860 ± 6 (50%)	86.0	Gly31	Gly88
P218A	47 ± 3 (7%)	66 ± 8 (8%)	88 ± 1 (9%)	66 ± 1 (4%)	886 ± 84 (51%)	18.9	Pro32	Pro89
H224R	650 ± 44 (92%)	852 ± 28 (98%)	651 ± 5 (67%)	1126 ± 25 (75%)	1462 ± 9 (85%)	2.3	His38	His95
G225A	270 ± 19 (38%)	257 ± 29 (30%)	237 ± 2 (24%)	326 ± 3 (22%)	1163 ± 26 (67%)	4.3	Gly39	Gly96
G225V	9 ± 3 (1%)	24 ± 3 (3%)	39 ± 1 (4%)	16 ± 1 (1%)	726 ± 41 (42%)	80.7		
R228A	522 ± 2 (74%)	612 ± 8 (70%)	488 ± 14 (50%)	790 ± 16 (52%)	1306 ± 21 (76%)	2.5	Arg42	Arg99
R228K	579 ± 3 (82%)	806 ± 18 (93%)	592 ± 19 (61%)	817 ± 19 (54%)	1386 ± 10 (80%)	2.4		
G235A	711 ± 2 (101%)	1031 ± 26 (118%)	845 ± 14 (88%)	1364 ± 69 (90%)	1663 ± 21 (96%)	2.3	Gly49	Gly106
G235V	353 ± 2 (50%)	452 ± 7 (52%)	345 ± 8 (35%)	545 ± 12 (36%)	1063 ± 8 (62%)	3.0		
E236A	99 ± 5 (14%)	130 ± 1 (15%)	249 ± 2 (26%)	274 ± 1 (18%)	1779 ± 15 (103%)	18.0	Glu50	Glu107
E236D	370 ± 4 (52%)	652 ± 17 (75%)	448 ± 11 (46%)	711 ± 6 (47%)	1223 ± 15 (71%)	3.3		
H249A	92 ± 3 (13%)	159 ± 1 (18%)	125 ± 1 (13%)	166 ± 1 (11%)	405 ± 5 (24%)	4.4	His63	Leu120
H249K	31 ± 1 (4%)	60 ± 8 (7%)	58 ± 1 (6%)	68 ± 1 (5%)	441 ± 32 (26%)	14.2		
G251A	635 ± 2 (90%)	917 ± 13 (105%)	781 ± 13 (82%)	1228 ± 22 (81%)	1561 ± 19 (91%)	2.5	Gly65	Gly122
G251V	297 ± 5 (42%)	452 ± 13 (51%)	342 ± 8 (35%)	561 ± 18 (37%)	1148 ± 30 (67%)	3.9		
R270A	25 ± 2 (4%)	28 ± 1 (3%)	42 ± 1 (4%)	23 ± 1 (2%)	810 ± 12 (47%)	32.4	Arg84	Arg141
R270 K	400 ± 6 (57%)	521 ± 11 (60%)	443 ± 16 (45%)	606 ± 13 (40%)	1334 ± 12 (77%)	3.3		
Y273A	19 ± 3 (3%)	28 ± 5 (3%)	70 ± 1 (7%)	90 ± 1 (6%)	1137 ± 15 (66%)	59.8	Tyr87	Tyr144
Y273W	34 ± 1 (5%)	19 ± 1 (2%)	74 ± 3 (8%)	50 ± 3 (3%)	1033 ± 11 (60%)	30.4		
Y273F	120 ± 23 (17%)	201 ± 27 (23%)	258 ± 5 (27%)	405 ± 17 (27%)	1303 ± 8 (76%)	10.9		
E288Q	28 ± 4 (4%)	48 ± 2 (6%)	56 ± 5 (6%)	73 ± 3 (5%)	499 ± 16 (29%)	17.8	Glu102	Glu159
E288D	14 ± 2 (2%)	29 ± 1 (3%)	77 ± 1 (8%)	101 ± 5 (7%)	246 ± 22 (14%)	17.6		
R298A	600 ± 30 (85%)	846 ± 34 (97%)	755 ± 20 (78%)	1256 ± 67 (83%)	1341 ± 17 (78%)	2.2	Arg112	Arg169
R298 K	742 ± 10 (105%)	889 ± 71 (102%)	896 ± 16 (92%)	1429 ± 17 (95%)	1623 ± 39 (94%)	2.2		
E308Q	22 ± 2 (3%)	58 ± 4 (7%)	47 ± 1 (5%)	44 ± 22 (3%)	324 ± 6 (19%)	14.7	Glu122	Glu179
E308D	580 ± 1 (82%)	831 ± 43 (95%)	782 ± 11 (80%)	1209 ± 9 (80%)	1407 ± 33 (82%)	2.4		
R311A	17 ± 2 (2%)	28 ± 1 (3%)	32 ± 18 (3%)	85 ± 1 (6%)	514 ± 1 (30%)	30.2	Arg125	Arg182
R311K	343 ± 28 (49%)	396 ± 28 (45%)	402 ± 23 (41%)	648 ± 24 (43%)	845 ± 6 (49%)	2.5		
H315A	604 ± 1 (86%)	921 ± 62 (106%)	814 ± 31 (84%)	1416 ± 33 (94%)	1417 ± 32 (82%)	2.3	His129	His186
H315R	209 ± 38 (30%)	296 ± 72 (34%)	373 ± 5 (38%)	653 ± 8 (43%)	808 ± 6 (47%)	3.9		
D325A	307 ± 32 (43%)	490 ± 13 (56%)	410 ± 14 (42%)	533 ± 2 (35%)	1586 ± 52 (92%)	5.2	Asp139	Asp196
D325E	445 ± 2 (63%)	536 ± 9 (62%)	529 ± 4 (54%)	599 ± 5 (40%)	1498 ± 21 (87%)	3.4		
H355A	92 ± 3 (13%)	246 ± 3 (28%)	162 ± 11 (17%)	221 ± 8 (15%)	1350 ± 17 (74%)	14.7	His169	His226
H355K	320 ± 1 (45%)	449 ± 14 (52%)	346 ± 6 (36%)	410 ± 4 (27%)	1175 ± 9 (68%)	3.7		
R556A	59 ± 5 (8%)	99 ± 6 (11%)	135 ± 1 (14%)	130 ± 1 (9%)	687 ± 39 (40%)	11.6	Lys369	Lys 426
R596A	340 ± 14 (48%)	486 ± 28 (56%)	455 ± 1 (47%)	612 ± 2 (41%)	1053 ± 44 (61%)	3.1	Arg409	Arg466

[a]Activity in nmol dNADH/mg protein/min. [b]Activity in nmol $K_3Fe(CN)_6$/mg protein/min. [c]Ratio of dNADH-$K_3Fe(CN)_6$ activity/dNADH-O_2 activity. [d]Corresponding residue in the Nqo4 subunit of *T. thermophilus*. [e]Corresponding residue in the 49 kDa subunit of *Y. lipolytica*.

Thus, differences in the dNADH-$K_3Fe(CN)_6$ reductase activity can be ascribed to different levels of enzyme found in the membrane fraction, that is, differences due to disrupted assembly. Table 1 includes dNADH-$K_3Fe(CN)_6$ reductase activity of all mutants together with the wild-type. The NuoD-KO mutant retained dNADH-$K_3Fe(CN)_6$ reductase activity of about 24% as compared to the wild-type, which is slightly lower than NuoC-KO mutant (36% of dNADH-$K_3Fe(CN)_6$ reductase activity).[38] As shown in Table 1, the KO-rev mutant displayed properties identical to that of the wild-type strain in all the enzymatic activities tested. Different point mutants analyzed displayed various reduced levels of dNADH-$K_3Fe(CN)_6$ reductase activity. In Table 1, we show the ratio of the dNADH-$K_3Fe(CN)_6$ reductase activity to the dNADH oxidase activity as an index to evaluate the specific effect of mutation on the Q reductase activity. The most drastic result was seen for His249, Glu288, Glu308, and Arg311 residues. Mutation of either Glu288 residue (to Q or D) or His249 (to A or K) resulted in ∼75% reduction in the activities comparable with the NuoD-KO mutant. Mutation of Glu308 (to Q) and Arg311 (to A) led to 70−80% reduction in the activities, while exchanging them with similar polar residue (E308D and R311K) barely affected the ferricyanide activity, suggesting their mutual ionic interaction, proposed by the X-ray structural model, is critical for the architecture. Mutations of Gly217, Pro218, Gly225, Arg270, His315, and Arg556 (to G217V, P218A, G225V, R270A, H315R, and R556A, respectively) resulted in ∼40−60% reduction in activities. A smaller but still considerable reduction in the activities (∼60%) occurred with mutations at the Tyr273 and Arg596 positions (Y273A, Y273W, and R596A).

NDH-1 Subunit Expression and Assembly in *E. coli* NuoD Mutants. The effect of NuoD segment mutation on the subunit contents and architecture of NDH-1 were studied by Western blotting and BN-PAGE. Antibodies against the six peripheral subunits NuoB, NuoCD, NuoE, NuoF, NuoG, and

DOI: 10.1021/bi501403t
Biochemistry 2015, 54, 753−764

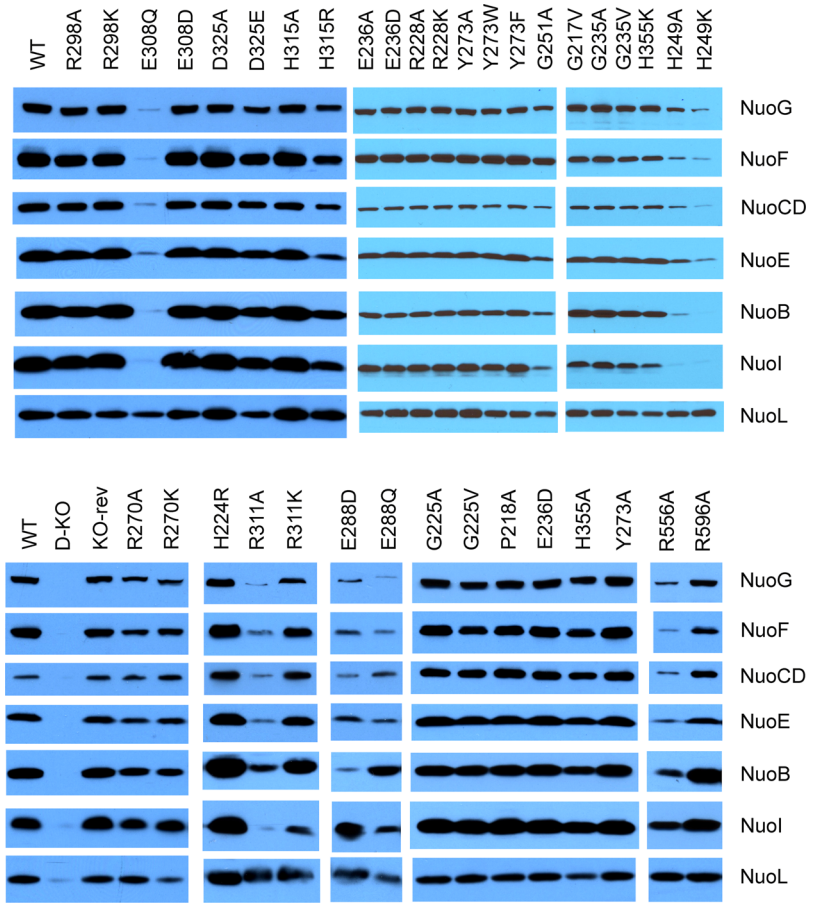

Figure 3. Immunoblotting of membrane preparations from wild-type (*WT*), NuoD knockout (*KO*), knockout revertant (*KO-rev*), and site-specific NuoD mutants. *E. coli* membranes (15 μg of protein per lane) were loaded on a 15% Laemmli SDS-polyacrylamide gel. After electrophoresis, the proteins were transferred onto nitrocellulose membranes, and Western blotting was carried out using the SuperSignal West Pico system. Antibodies specific to NuoB, NuoCD, NuoE, NuoF, NuoG, NuoI, and NuoL were used. Goat antirabbit IgG horseradish peroxidase conjugate was used as secondary antibody.

NuoI and membrane subunit NuoL were used in a systematic immunochemical analysis to examine the subunit contents of the NDH-1 in the membrane samples from all NuoD mutants. As seen in Figure 3, all the tested subunits were almost entirely missing in the membranes of NuoD knockout cells. This clearly indicates that NuoD is absolutely required for the assembly of the NDH-1 complex. In the revertant mutant (KO-rev), all tested subunits existed at the same levels as the wild-type, validating the process of chromosomal manipulation.

The enzymatic activities of NDH-1 of the mutants suggested that His249, Glu288, Glu308, and Arg311 are essential residues for the assembly. As expected, for several of the mutants of these residues including H249A, H249 K, E288Q, E288D, E308Q, and R311A, we observed significant and divergent quantitative differences for the seven NDH-1 subunits tested. All of the above-mentioned mutants had a relatively lower content for the hydrophilic subunits tested. The R556A mutant also showed rather low content of most of the tested peripheral subunits. R311K and H355K mutants showed slightly lower content of NuoI subunit as compared to the wild-type. Likewise, the mutant H315R showed slightly lower content of the NuoE subunit. A majority of the other NuoD domain mutants were found to contain similar amounts of the subunits tested when compared to the wild-type.

To directly verify the assembled NDH-1 in the mutants, we used BN-PAGE to analyze these membrane samples. After BN-PAGE, the amount of fully assembled complex was evaluated through NADH dehydrogenase activity staining. As shown in Figure 4, no intact NDH-1 was observed in the NuoD knockout mutant. In contrast, membranes isolated from the wild-type and NuoD KO-rev mutants seemed to contain similar amounts of fully assembled NDH-1. As seen in Figure 4, NDH-1 complex was destabilized for the mutations E288Q, E288D, and E308Q mutants. H249A, H249K, R311A, and R556A mutants displayed greatly diminished level of the assembled complex substantiating the fact that they had low dNADH-$K_3Fe(CN)_6$ activity, while the R311K and H355A mutations showed a slight decrease in the amount of the assembled NDH-1. Membranes from most of the other mutants contained fully assembled NDH-1 comparable to that of wild-type. The results are mostly in good agreement with the data obtained from the immunoblotting and assay of dNADH-$K_3Fe(CN)_6$ reductase activity.

Taken together, our results indicate that drastic changes altered the assembly status of the NDH-1 in some of the point mutants of NuoD segment (H249A, H249K, E288D, E288Q, E308Q, R311A, and R556A in particular) constructed in this study. The roles of these residues can be explained as follows: Glu308 and Arg311 are located in the longest helix in the NuoD segment and interact with Arg435 (Figure 5a). Also, the highly conserved Arg303 (not mutated in this study) most likely interacts with Glu288 (Figure 5b). Thus, the results from

DOI: 10.1021/bi501403t
Biochemistry 2015, 54, 753−764

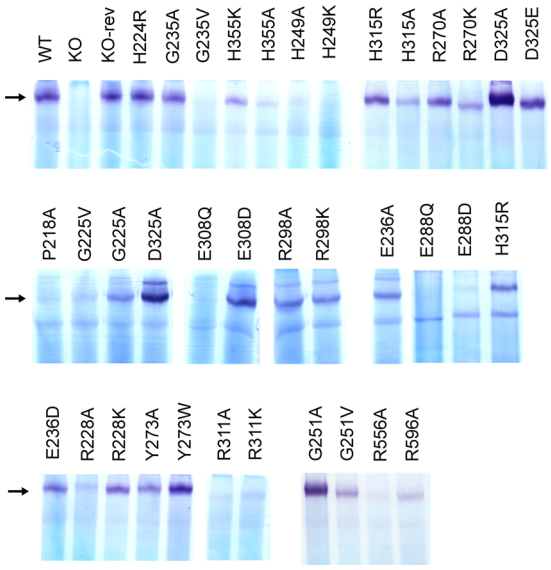

Figure 4. BN-PAGE of membrane preparations of the NuoD mutants. 1.0% *n*-Dodecyl-*β*-D-maltoside was used for the extraction of NDH-1 from the membrane samples. The gels were incubated for 1 h with 2.5 *μ*g/mL *ρ*-nitroblue tetrazolium and 0.15 mM NADH in 2 mM Tris buffer (pH 7.5) at 37 °C. The reaction was stopped by 7% acetic acid. The arrows show the location of the NDH-1 band.

these mutations suggest that the structure of the longest helix in the NuoD segment is vital for the whole structural integrity of NDH-1. His249 in NuoD and Tyr139 in NuoB are most likely close enough to interact with each other. The corresponding residues in the *T. thermophilus* structure are spaced at a distance of 2.8 Å (same for the calculated distance in our homology modeling of the *E. coli* NDH-1) (Figure 5c). They seem to contribute to the structural integrity of the subunits. Also, the C terminal residues Arg556 and Arg596 were predicted to be located at a distance of within 3 Å from Glu136 in the NuoC segment in our previous superimposition of the *E. coli* NDH-1 model onto the *T. thermophilus* structure.[38] In our homology modeling of the *E. coli* NDH-1 from recent *T. thermophilus* structure,[22] it is suggested that Arg556 may also be close (calculated to be 2.5 Å) from the highly conserved Glu253 (Figure 5d). The impaired NDH-1 assembly by the R556A mutation compared to that of the R596A mutant accounts for the specific interaction of Glu253 with Arg556.

Measurements of NDH-1 Activities in NuoD Mutants. dNADH oxidase and dNADH-UQ-oxidoreductase activities of NDH-1 were measured in *E. coli* membrane vesicles. Three different Q substrates with different side-chain length (namely, DB, UQ_1, and UQ_2) were used for this purpose along with dNADH for measuring NDH-1 specific activity. Table 1 lists data from point mutation studies on the NuoD segment, while Table 2 shows data from point mutation studies on the NuoH subunit that we had conducted earlier and reanalyzed in this work.[41] The dNADH oxidase and dNADH-Q (dNADH-DB, dNADH-UQ_1, and dNADH-UQ_2) reductase activity were affected to different degrees among the different NuoD domain mutants. We observed that these activities generally behaved in a parallel fashion among the majority of the mutants.

Although in some regions of the NuoD segment different exchanges had comparatively severe effects on the activity, only some of the mutations markedly reduced activity in other parts of the protein. As expected, the energy-transducing NDH-1 activities were almost completely abolished for the H249A, H249K, E288Q, E288D, E308Q, R311A, and R556A mutants

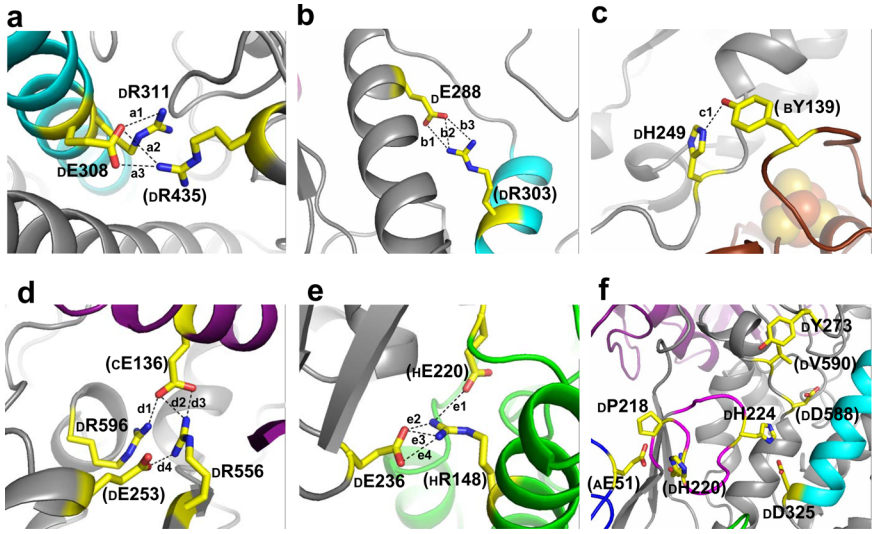

Figure 5. Visualization of the interaction of key charged residues for the activity or assembly in the homology model of *E. coli* NuoD and the neighboring subunits. Near-neighbor relationships of the charged residues mutated in this study were examined. Residues that were estimated to be within 3 Å in the *E. coli* model are connected with dashed lines in the figure. The distances calculated based on the modeled structure are given below (in Å). For comparison, the corresponding values obtained from the *T. thermophilus* 3D structure are provided in square brackets (in Å). (a) Glu308 and Arg311 in the long *α* helix of NuoD: a1 = 3.3 [3.3]; Glu308 and Arg435 of NuoD: a2 = 3.3 [3.3], a3 = 2.7 [2.6] (b) Arg303 in the long *α* helix of NuoD and Glu288 of NuoD: b1 = 3.4 [3.4], b2 = 3.0 [2.8], b3 = 3.4 [3.4]. (c) His249 of NuoD and Tyr139 of NuoB: c1 = 2.8 [2.8]. (d) Arg596 of NuoD and Glu136 of NuoC: d1 = 2.6 [2.6]. Glu136 of NuoC and Arg556 of NuoD: d2 = 2.5, d3 = 2.1 [no corresponding residue for Arg556]. Glu253 and Arg556 of NuoD: d4 = 2.5 [no corresponding residue for Arg556]; (e) Arg148 and Glu220 of NuoH: e1 = 3.4 [3.1]; Arg148 of NuoH and Glu236 of NuoD: e2 = 2.2 [2.4], e3 = 2.4 [2.6], e4 = 2.9 [2.8]. (f) Pro218 in the conserved loop of NuoD and Glu51 of the NuoA subunit; His224 in the conserved loop and Asp325 of NuoD. The 3D model for each subunit was obtained as given in Figure 2. Visualization and distance measurements were carried out using PyMOL ver. 1.7.2.[63] Residues that were not examined in this work are shown in parentheses.

DOI: 10.1021/bi501403t
Biochemistry 2015, 54, 753−764

Table 2. Enzymatic Activities of the Wild-Type and Various NuoH Mutants of *E. coli* NDH-1

mutant	dNADH-O_2[a,b]	dNADH-DB[a,b]	dNADH-UQ_1[b]	dNADH-UQ_2[b]	dNADH-$K_3Fe(CN)_6$[a,c]
WT	723 ± 33 (100%)	1041 ± 35 (100%)	973 (100%)	1508 (100%)	1367 ± 24 (100%)
E36D	559 ± 52 (77%)	539 ± 16 (52%)	998 (103%)	1167 (77%)	1015 ± 47 (74%)
Q44A	325 ± 38 (45%)	561 ± 23 (54%)	705 (72%)	1137 (75%)	1658 ± 11 (121%)
P49A	424 ± 19 (59%)	402 ± 15 (39%)	806 (83%)	1168 (77%)	1063 ± 42 (78%)
D63E	642 ± 91 (89%)	964 ± 65 (93%)	885 (91%)	1103 (73%)	1536 ± 37 (112%)
E71A	348 ± 25 (48%)	388 ± 9 (37%)	634 (65%)	855 (57%)	987 ± 17 (72%)
E157K	804 ± 66 (111%)	838 ± 43 (80%)	613 (63%)	950 (63%)	2190 ± 103 (160%)
E216A	668 ± 43 (92%)	837 ± 21 (80%)	611 (63%)	940 (62%)	1532 ± 40 (112%)
K303A	338 ± 36 (47%)	657 ± 32 (63%)	728 (75%)	897 (59%)	974 ± 74 (71%)

[a]Data taken from ref 41. [b]Activity in nmol dNADH/mg protein/min. [c]Activity in nmol $K_3Fe(CN)_6$/mg protein/min.

that earlier showed very low ferricyanide activity along with highly reduced subunit contents and lack of NDH-1 assembly. Significant reductions in the activity were also observed for the mutation of residues in the possible Q biding site or near cluster N2 (G217V, P218A, G225V, R270A, Y273A, Y273W, and H355A). These mutants had moderately reduced ferricyanide activity, showing higher ratios of dNADH-$K_3Fe(CN)_6$ reductase activity/NADH oxidase activity (Table 1). It should be noted that Y273F showed slightly better activity (20−30%) than that of Y273A and Y273W (less than 10%), which is somewhat different from the mutational study of the corresponding Tyr144 in *Y. lipolytica* 49 kDa subunit.[50]

Glu236 is well-conserved, and the corresponding position in human 49K subunit is associated with Leigh Syndrome.[51] According to the X-ray structure of *T. thermophilus* NDH-1, Glu50 in a loop of Nqo4 (Glu236 of NuoD) interacts with Arg154 and Glu227 in Nqo8 (Arg148 and Glu220 in the NuoH subunit, respectively), forming connection points to the cytoplasm.[22] The same interaction was observed in the homology modeling of *E. coli* NDH-1 (Figure 5e). Mutation of Glu236 to Ala resulted in diminished activities (15−20%), while exchanging this acidic residue for another acidic residue Asp largely retained the activity (in the range of 50% as compared to the wild-type; dNADH-DB activity was relatively high at, i.e., 75%).

Less drastic but still significant diminution of the energy-transducing NDH-1 activity was observed for the mutations of Asp325 to Ala or Glu, which has ionic interaction with His224 (Figure 5f). A considerably reduced energy transducing NDH-1 activity was also observed in G225A, H315R, D325A, D325E, and R596A, reflecting the diminished level of assembly of NDH-1 in the mutants. The dNADH oxidase, dNADH-DB, dNADH-UQ_1, and dNADH-UQ_2 reductase activities of other NuoD mutants including R228A, R228K, and H224R were mostly comparable to that of the wild-type.

Effects of NuoD Mutations on IC_{50} of NDH-1 Inhibitors. Various complex I inhibitors are considered to act on the same Q binding cavity with different but partially overlapping sites. Murai et al. used a photoreactive AzQ and showed that the interface between 49 kDa (NuoD) and ND1 (NuoH) subunits forms the inhibitor/Q binding cavity[52] (Figure 2a). A similar result was obtained using acetogenins.[27,53] Capsaicin-40 (Cap-40) acts as a competitive inhibitor for Q in NDH-1/complex I and suppresses only energy-coupled activities.[54] We measured the IC_{50} values for three inhibitors, azidoquinazoline (AzQ), squamotacin (one of the acetogenins), and capsaicin-40 using our NuoD and NuoH mutants of NDH-1.

The mutation of G225A caused about 5-fold increase in the IC_{50} value for Cap-40 (Table 3). Similarly, the IC_{50} value of AzQ for the G225A mutant was also increased by ∼3-fold (Table 4). The Y273F mutant exhibited insensitivity toward Cap-40, while a ∼2.5-fold increase in the IC_{50} value for AzQ was observed for the same mutant. A considerable increase (about 5-fold) in the IC_{50} value was observed only for capsaicin-40 and not for AzQ for the mutant D325A. For all other NuoD mutants, IC_{50} values were determined to be in the range of 0.11−0.18 μM for Cap-40 and 1000 nM for AzQ

Table 3. Inhibitor Sensitivities (Capsaicin-40, AzQ and Squamotacin) of the Wild-Type and Various NuoD Mutants of *E. coli* NDH-1

mutant	app IC_{50} (capsaicin-40)[a]	app IC_{50} (AzQ)[b]	app IC_{50} (squamotacin)[c]
WT	129	1078	10
KO-rev			
H224R	166	1134	
G225A	650	3008	5
R228A	167	1106	2
R228K	158	1211	3
G235A	115	1175	4
G235V	141	934	6
E236A	185		5
E236D	113	920	7
G251A	158	1222	4
G251V	133	951	2
H249A	138		
R270K	81	980	2
Y273F	insensitive	2529	9
R298A	91	784	2
R298K	73	954	4
E308D	93	966	2
R311K	70	815	4
H315A	134	992	10
H315R	202	903	4
D325A	585	1137	11
D325E	183	999	5
H355A	163	711	5
H355K	126	1117	
R596A	113	759	

[a]The concentration of capsaicin-40 (in nM) that causes 50% inhibition of the dNADH oxidase activity. [b]The concentration of AzQ (in nM) that causes 50% inhibition of the dNADH oxidase activity. [c]The concentration of Squamotacin (in nM) that causes 50% inhibition of the dNADH oxidase activity.

DOI: 10.1021/bi501403t
Biochemistry 2015, 54, 753−764

Table 4. Inhibitor Sensitivities (Capsaicin-40, AzQ, and Squamotacin) of the Wild-Type and Various NuoH Mutants of *E. coli* NDH-1

mutant	app IC_{50} (capsaicin-40)[a]	app IC_{50} (AzQ)[b]	app IC_{50} (squamotacin)[c]
WT	151	1078	10
E36D	95	293	3
Q44A	85	676	5
P49A	115	593	5
D63E	92	271	4
E71A	159	559	3
E157K	98	692	6
E216A	95	647	8
K303A	199	691	10

[a]The concentration of capsaicin-40 (in nM) that causes 50% inhibition of the dNADH oxidase activity. [b]The concentration of AzQ (in nM) that causes 50% inhibition of the dNADH oxidase activity. [c]The concentration of squamotacin (in nM) that causes 50% inhibition of the dNADH oxidase activity.

(Table 3), suggesting that the Cap-40 and AzQ binding site was not modified by these point mutations.

Acetogenin (e.g., asimicin and squamotacin) is one of the most potent inhibitors for *E. coli* NDH-1 with an IC_{50} value of 2−10 nM.[16,55] In the present work, we used squamotacin and investigated the effects of NuoD mutations on the inhibitory characteristics. The IC_{50} values of squamotacin for mutants R228A, R228 K, G251V, R270K, R298A, and E308D of the NuoD segment were somewhat lower (2−3 nM) as compared to the wild-type (10 nM). For most of the other mutants IC_{50} was determined to be in the range of 5.0−10 nM.

Analysis of NuoH Mutations. In an earlier study on the NuoH subunit, many of the residues in the cytoplasmic hydrophilic segments of the subunit affected the NDH-1 assembly.[41] In the present work, we focused only on the mutations that scarcely affected the assembly (Table 2), by reinvestigating the sensitivity of inhibitors. As seen in Table 4, none of the mutants drastically altered the capsaicin binding cavity for the NuoH mutants. In contrast, several of the NuoH mutants exhibited a slight hypersensitivity for AzQ. Among them, noticeably, mutants E36D and D63E showed ∼3−4 fold decrease in the IC_{50} value for AzQ. Similarly, the IC_{50} value of Squamotacin for E36D, D63E, and E71A mutants was lower (3−4 nM) as compared to the wild-type (10 nM).

Proton Translocation by NuoCD Mutants. We monitored the generation of proton gradient (ΔpH, inside acidic) in membrane vesicles of the NuoD mutants using ACMA as reporter and dNADH as substrate. Representative traces are shown in Supplemental Figure 2, Supporting Information. Membrane vesicles from wild-type and the KO-rev mutant exhibited almost identical response with a maximum quenching seen after addition of dNADH. The addition of FCCP completely reversed the signal. As expected, no proton gradient was observed for the membranes vesicles of the NuoD-KO mutant. Similarly, no proton translocation activity was observed in the G225V and E308Q mutants. Likewise, mutants E288Q, E288D, and H355A did not show an appreciable sign of proton pumping activity. Membranes from Y273A, R270A, R311A, H315R, and E236D had significantly lower fluorescence quenching, whereas those from G225A, D325A, and R311K exhibited moderate fluorescence quenching, with D325E, R556A, and R270K showing a slightly enhanced quenching. Mutants H224R, G251A, and R298 K all displayed wild-type-like fluorescence quenching. R228A, R228K, R298A, E308D, and G235A mutants had only a little lower fluorescence quenching as compared to the wild-type.

Similar results were obtained in the membrane potential (ΔΨ) analysis with the membrane vesicles of the NuoD mutants using oxonol VI. Membrane vesicles of the wild-type showed a maximum ΔΨ after the addition of dNADH, and FCCP totally abolished the ΔΨ. No ΔΨ was generated in the case of NuoD-KO mutant. The representative traces from a few key mutants are shown in Supplemental Figure 3, Supporting Information.

DISCUSSION

Analysis of the X-ray data of *T. thermophilus* NDH-1 with Q suggested that Tyr87 and His38 of the Nqo4 subunit (Tyr273 and His224 of NuoD) directly interact with the Q headgroup.[22] Our mutational study demonstrated the significance of the conserved Tyr273 with the Y273F mutant retaining a partial activity. Interestingly, this activity was not inhibitable by Cap-40 and showed a reduced sensitivity to AzQ, suggesting that these inhibitors interact with Tyr273. The result agrees with the earlier investigation of the corresponding residue, Tyr144 in *Y. lipolytica*.[30,50] On the other hand, because the sensitivity to squamotacin was unchanged, the residue is probably not involved in the binding of acetogenins. Mutation of His224 yielded varied results. Our mutant, H224R, had activity similar to that of the wild-type, indicating that this highly conserved histidine is probably not required for the Q reduction. Its alanine mutant was reported to have the same result.[47] On the other hand, the earlier work with the 49 kDa of *Y. lipolytica* implied that His95 (His224 of NuoD) is critical for activity.[46] Whether this is due to a species difference remains to be seen.

A highly conserved loop between the first and second beta-sheet near the N-terminus of the NuoD segment (Gly217−Phe227, see Figure 2) seems to bear important functional and structural roles. According to the 3D model, the loop could be divided into two regions. One region, Ser222 to Phe227, faces the Q binding cavity and has the aforementioned His224. There is a highly conserved Gly225 located next to His224. Mutation of this glycine to valine totally abolished the energy-transducing NDH-1 activity. When it was mutated to alanine, about 30% of the activity was observed, and the mutation conferred the resistance to Cap-40 and AzQ. Thus, it seems that the area around His224 and Gly225 in the loop is structurally important as part of the Q binding cavity. The other region of the loop (Gly217−Pro221) may bear a more distinct structural role. This region is adjacent to a cytoplasmic loop (Phe50−Asp55) between the first and second transmembrane segments of the NuoA subunit (Figures 2a and 5f). His220 in the NuoD loop and highly conserved Glu51 in the NuoA loop are seemingly close enough to have an ionic interaction (Figure 5f). On the basis of the observation made with selective chemical modification of the deactive form of complex I,[56] Sazanov proposed that this cytoplasmic loop in NuoA partially prevents solvent from accessing the Q cavity and thus is important for activity.[22,57] We can envisage that the two loops share the same role, and their structural integrity might be crucial for the enzyme reaction. Mutation of Glu51 in the NuoA loop led to a significant loss of the activity.[14] Also, the complete loss of activity observed with mutation of G217 and P218 in the NuoD loop could be due to a breakage in the structure of the loop. Glycine and proline are both known to

DOI: 10.1021/bi501403t
Biochemistry 2015, 54, 753−764

play structural roles as seen, for example, in the GxGxxG motif.[58]

A higher resistance to Cap-40 compared to the wild-type was also observed in the D325A mutant. Miyoshi's group demonstrated that an acetogenin that has an alkynylated tosylate in the tail interacts with Asp160 in the bovine 49 kDa subunit (Asp325 of *E. coli* NuoD).[27] Our mutagenesis result of D325A/E agrees with the result that the alkynylation of the aspartic acid markedly decreases the activity of complex I. V407M (*E. coli* V590) mutation in the C-terminal part of the NuoD subunit of *Rhodobacter capsulatus* was found to be resistant to piericidin as well as to rotenone.[59] Mutations of the neighboring conserved residue Asp458 (*E. coli* Asp588) to alanine in *Y. lipolytica* 49-kDa subunit was also shown to cause resistance to rotenone and Q-analogue inhibitor 2-decyl-4-quinazolinyl amine.[28] It is conceivable that the conserved loop including the region around the interaction of His224 and Asp325, along with the C-terminal part presumably forms a narrow Q cavity where most of the NDH-1 inhibitors are believed to bind (Figure 5f).

Our present result showed that several of the NuoH mutants, including E36D and D63E in the cytoplasmic side exhibited slight hypersensitivity for the inhibitor AzQ. It was recently reported that mutations of the Glu36 in *E. coli* NuoH decreased the apparent affinity of the enzyme to Q as well as partially competitive inhibitors and induced resistance to stigmatellin, a less specific inhibitor.[60] The E36Q mutation in *E. coli* NuoH affected the kinetics of all tested Q species and also affected UQ and inhibitor binding to a similar extent.[60] These results may be related to the fact that Glu36 and Asp63 are located on the cytoplasmic side of NuoH that is considered to contribute to the putative Q binding cavity.

It was interesting to observe that a significant number of mutations led to increased sensitivity to squamotacin. One can imagine that such mutations resulted in destabilized complex I, which would lead to rather "relaxed" structure, at least partly. It is likely that such "relaxed" structures would allow for easier access of the long and bulky squamotacin into the enclosed Q-binding site.

The Glu236 residue in another loop of the NuoD segment and Arg148 and Glu220 of the NuoH subunit are indispensable and interacting with each other, possibly forming connection points toward the cytoplasm[22] (Figure 5e). Earlier, Arg148 and Glu220 residues in the NuoH subunit were found to be important for both the energy-transducing activity and assembly of NDH-1.[41] Notably, they are located adjacent to the above-mentioned loops in NuoD and NuoA that likely protect the Q cavity form the solvent access. Hence, together with the X-ray structure, we predict a probable connection to the cytoplasm for proton translocation lies around these charged residues, which also play structural roles, keeping together subunits and loops, thus enclosing the Q cavity beneath them.

The four α-helical bundle in the NuoD segment seemingly plays a role in some conformational change in the peripheral domain of NDH-1,[61] or at least, the backbone of the Q binding cavity.[29] Of these, our mutational study in the longest helix suggested its structural roles by indispensable ionic interaction of Glu308-Arg311-Arg435 and Glu288-Arg311 (Figure 5a,b). As Asp325 in the same helix is close to the aforementioned conserved loop, this structurally critical helix could be involved in the energy transduction by responding to the Q reduction.

The deleterious effect of mutation in His249 on the assembly strongly indicated its interaction with highly conserved Tyr139 in NuoB, which is indispensable for the stability of NDH-1 (Figure 5c). The ionic interactions among Arg556, Arg596, and Glu253 of NuoD and Glu136 of NuoC also contribute to the structural integrity of the NuoCD subunit (Figure 5d). Strikingly, these key contact residues in NuoB, NuoC, and NuoD are close to each other, lying immediately above and almost in the same plane as the Q binding cavity (Figure 2a).

The present results all together strongly suggest that the NuoD segment is a "core of the core" region in the NDH-1 where the substrate Q and the majority of NDH-1/complex I inhibitors bind. The tight shield of the Q cavity from the solvent and the structural intactness of the subunit are absolutely imperative for the function of the enzyme.

■ ASSOCIATED CONTENT

Ⓢ Supporting Information

Figures S1−S3. This material is available free of charge via the Internet at http://pubs.acs.org.

■ AUTHOR INFORMATION

Corresponding Author

*Phone: 858-784-8094. E-mail: yagi@scripps.edu.

Present Addresses

○Pennsylvania State University, College of Medicine, Hershey, Pennsylvania.

⊥Life Sciences Center, University of Missouri, Columbia, Missouri.

▽Department of Pharmacological and Pharmaceutical Sciences, University of Houston, Texas.

‖Odawara Research Center, Nippon Soda Co., Ltd., Odawara 250-0280, Japan.

◇Centro de investigaciones Biologicas del CSIC, Madrid, 28040 Madrid, Spain.

□Lab of Molecular and Cellular Neuroscience, The Rockefeller University, 1230 York Ave, New York, NY 10065.

Author Contributions

#These authors equally contributed to this work.

Funding

This work was supported by NIH Grant R01 GM033712 (to T.Y. and A.M.-Y.).

Notes

The authors declare no competing financial interest.

■ ACKNOWLEDGMENTS

We thank Dr. Jennifer Barber-Singh (The Scripps Research Institute) for critical reading of the manuscript. We also thank anonymous reviewers for helpful suggestions, which helped significantly in improving the presentation.

■ ABBREVIATIONS:

Q, quinone; complex I, mitochondrial proton-translocating NADH-quinone oxidoreductase; NDH-1, bacterial proton-translocating NADH-quinone oxidoreductase; DB, 2,3-dimethoxy-5-methyl-6-decyl-1,4-benzoquinone; UQ_1, ubiquinone-1; UQ_2, ubiquinone-2; AzQ, 6-azido-4-(4-iodophenetylamino)-quinazoline; dNADH, reduced nicotinamide hypoxanthine dinucleotide; oxonol VI, bis(3-propyl-5-oxoisoxazol-4-yl)-pentamethine oxonol; ACMA, 9-amino-6-chloro-2-methoxyacridine; FCCP, carbonyl cyanide *p*-trifluoromethoxy phenyl-

DOI: 10.1021/bi501403t
Biochemistry 2015, 54, 753−764

hydrazone; BN-PAGE, blue native polyacrylamide gel electrophoresis

REFERENCES

(1) Yagi, T., and Matsuno-Yagi, A. (2003) The proton-translocating NADH-quinone oxidoreductase in the respiratory chain: The secret unlocked. *Biochemistry 42*, 2266−2274.

(2) Brandt, U. (2006) Energy Converting NADH:Quinone Oxidoreductase (Complex I). *Annu. Rev. Biochem. 75*, 69−92.

(3) Carroll, J., Fearnley, I. M., Skehel, J. M., Shannon, R. J., Hirst, J., and Walker, J. E. (2006) Bovine complex I is a complex of forty-five different subunits. *J. Biol. Chem. 281*, 32724−32727.

(4) Balsa, E., Marco, R., Perales-Clemente, E., Szklarczyk, R., Calvo, E., Landazuri, M. O., and Enriquez, J. A. (2012) NDUFA4 Is a Subunit of Complex IV of the Mammalian Electron Transport Chain. *Cell Metab. 16*, 378−386.

(5) Sinha, P. K., Castro-Guerrero, N., Matsuno-Yagi, A., Yagi, T., and Torres-Bacete, J. (2009) Bacterial complex I (NDH-1): Functional roles of the hydrophobic domain. *Curr. Topics Biochem. Res. 11*, 79−90.

(6) Yagi, T., Di Bernardo, S., Nakamaru-Ogiso, E., Kao, M. C., Seo, B. B., and Matsuno-Yagi, A. (2004) NADH Dehydrogenase (NADH-Quinone Oxidoreductase). In *Advances in Photosynthesis and Respiration; Respiration in Archaea and Bacteria* (Zannoni, D., Ed.) Vol. *15*, pp 15−40, Kluwer Academic Publishers, Dordrecht.

(7) Yagi, T., Yano, T., Di Bernardo, S., and Matsuno-Yagi, A. (1998) Procaryotic complex I (NDH-1), an overview. *Biochim. Biophys. Acta 1364*, 125−133.

(8) Efremov, R. G., and Sazanov, L. A. (2011) Respiratory complex I: 'steam engine' of the cell? *Curr. Opin. Struct. Biol. 21*, 532−540.

(9) Matsuno-Yagi, A., and Yagi, T. (2001) Introduction: complex I – an L-shaped black box. *J. Bioenerg. Biomembr. 33*, 155−157.

(10) Hinchliffe, P., and Sazanov, L. A. (2005) Organization of iron-sulfur clusters in respiratory complex I. *Science 309*, 771−774.

(11) Sazanov, L. A., and Hinchliffe, P. (2006) Structure of the Hydrophilic Domain of Respiratory Complex I from *Thermus thermophilus*. *Science 311*, 1430−1436.

(12) Friedrich, T. (2014) On the mechanism of respiratory complex I. *J. Bioenerg. Biomembr. 46*, 255−268.

(13) Kao, M. C., Di Bernardo, S., Nakamaru-Ogiso, E., Miyoshi, H., Matsuno-Yagi, A., and Yagi, T. (2005) Characterization of the membrane domain subunit NuoJ (ND6) of the NADH-quinone oxidoreductase from *Escherichia coli* by chromosomal DNA manipulation. *Biochemistry 44*, 3562−3571.

(14) Kao, M. C., Nakamaru-Ogiso, E., Matsuno-Yagi, A., and Yagi, T. (2005) Characterization of the membrane domain subunit NuoK (ND4L) of the NADH-quinone oxidoreductase from *Escherichia coli*. *Biochemistry 44*, 9545−9554.

(15) Kao, M. C., Di Bernardo, S., Perego, M., Nakamaru-Ogiso, E., Matsuno-Yagi, A., and Yagi, T. (2004) Functional roles of four conserved charged residues in the membrane domain subunit NuoA of the proton-translocating NADH-quinone oxidoreductase from *Escherichia coli*. *J. Biol. Chem. 279*, 32360−32366.

(16) Nakamaru-Ogiso, E., Kao, M. C., Chen, H., Sinha, S. C., Yagi, T., and Ohnishi, T. (2010) The membrane subunit NuoL (ND5) is involved in the indirect proton pumping mechanism of *E. coli* complex I. *J. Biol. Chem. 285*, 39070−39078.

(17) Torres-Bacete, J., Sinha, P. K., Castro-Guerrero, N., Matsuno-Yagi, A., and Yagi, T. (2009) Features of subunit NuoM (ND4) in *Escherichia coli* NDH-1: Topology and implication of conserved Glu144 for coupling site 1. *J. Biol. Chem. 284*, 33062−33069.

(18) Sato, M., Sinha, P. K., Torres-Bacete, J., Matsuno-Yagi, A., and Yagi, T. (2013) Energy transducing roles of antiporter-like subunits in *E. coli* NDH-1 with main focus on subunit NuoN (ND2). *J. Biol. Chem. 288*, 24705−24716.

(19) Efremov, R. G., and Sazanov, L. A. (2011) Structure of the membrane domain of respiratory complex I. *Nature 476*, 414−420.

(20) Efremov, R. G., Baradaran, R., and Sazanov, L. A. (2010) The architecture of respiratory complex I. *Nature 465*, 441−445.

(21) Hunte, C., Zickermann, V., and Brandt, U. (2010) Functional Modules and Structural Basis of Conformational Coupling in Mitochondrial Complex I. *Science 329*, 448−451.

(22) Baradaran, R., Berrisford, J. M., Minhas, G. S., and Sazanov, L. A. (2013) Crystal structure of the entire respiratory complex I. *Nature 494*, 443−448.

(23) Murai, M., Mashimo, Y., Hirst, J., and Miyoshi, H. (2011) Exploring Interactions between the 49 kDa and ND1 Subunits in Mitochondrial NADH-Ubiquinone Oxidoreductase (Complex I) by Photoaffinity Labeling. *Biochemistry 50*, 6901−6908.

(24) Murai, M., Ishihara, A., Nishioka, T., Yagi, T., and Miyoshi, H. (2007) The ND1 Subunit Constructs the Inhibitor Binding Domain in Bovine Heart Mitochondrial Complex I. *Biochemistry 46*, 6409−6416.

(25) Ohshima, M., Miyoshi, H., Sakamoto, K., Takegami, K., Iwata, J., Kuwabara, K., Iwamura, H., and Yagi, T. (1998) Characterization of the ubiquinone reduction site of mitochondrial complex I using bulky synthetic ubiquinones. *Biochemistry 37*, 6436−6445.

(26) Sekiguchi, K., Murai, M., and Miyoshi, H. (2009) Exploring the binding site of acetogenin in the ND1 subunit of bovine mitochondrial complex I. *Biochim. Biophys. Acta 1787*, 1106−1111.

(27) Masuya, T., Murai, M., Ifuku, K., Morisaka, H., and Miyoshi, H. (2014) Site-specific chemical labeling of mitochondrial respiratory complex I through ligand-directed tosylate chemistry. *Biochemistry 53*, 2307−2317.

(28) Kashani-Poor, N., Zwicker, K., Kerscher, S., and Brandt, U. (2001) A central functional role for the 49 kDa subunit within the catalytic core of mitochondrial complex I. *J. Biol. Chem. 276*, 24082−24087.

(29) Tocilescu, M. A., Fendel, U., Zwicker, K., Kerscher, S., and Brandt, U. (2007) Exploring the ubiquinone binding cavity of respiratory complex I. *J. Biol. Chem. 282*, 29514−29520.

(30) Tocilescu, M. A., Zickermann, V., Zwicker, K., and Brandt, U. (2010) Quinone binding and reduction by respiratory complex I. *Biochim. Biophys. Acta 1797*, 1883−1890.

(31) Zickermann, V., Kerscher, S., Zwicker, K., Tocilescu, M. A., Radermacher, M., and Brandt, U. (2009) Architecture of complex I and its implications for electron transfer and proton pumping. *Biochim. Biophys. Acta 1787*, 574−583.

(32) Earley, F. G. P., Patel, S. D., Ragan, C. I., and Attardi, G. (1987) Photolabelling of a mitochondrially encoded subunit of NADH dehydrogenase with [^{3}H]dihydrorotenone. *FEBS Lett. 219*, 108−113.

(33) Ichimaru, N., Murai, M., Kakutani, N., Kako, J., Ishihara, A., Nakagawa, Y., Nishioka, T., Yagi, T., and Miyoshi, H. (2008) Synthesis and Characterization of New Piperazine-Type Inhibitors for Mitochondrial NADH-Ubiquinone Oxidoreductase (Complex I). *Biochemistry 47*, 10816−10826.

(34) Sinha, P. K., Nakamaru-Ogiso, E., Torres-Bacete, J., Sato, M., Castro-Guerrero, N., Ohnishi, T., Matsuno-Yagi, A., and Yagi, T. (2012) Electron Transfer in subunit NuoI (TYKY) of *Escherichia coli* NDH-1 (NADH:quinone oxidoreductase). *J. Biol. Chem. 287*, 17363−17373.

(35) Torres-Bacete, J., Nakamaru-Ogiso, E., Matsuno-Yagi, A., and Yagi, T. (2007) Characterization of the NuoM (ND4) subunit in *Escherichia coli* NDH-1: Conserved charged residues essential for energy-coupled activities. *J. Biol. Chem. 282*, 36914−36922.

(36) Sato, M., Torres-Bacete, J., Sinha, P. K., Matsuno-Yagi, A., and Yagi, T. (2014) Essential regions in the membrane domain of bacterial complex I (NDH-1): the machinery for proton translocation. *J. Bioenerg. Biomembr. 46*, 279−287.

(37) Yagi, T., Torres-Bacete, J., Sinha, P. K., Castro-Guerrero, N., and Matsuno-Yagi, A. (2012) in *A Structural Perspective on Respiratory Complex I* (Sazanov, L., Ed.) pp 147−169, Springer, Chambersburg.

(38) Castro-Guerrero, N., Sinha, P. K., Torres-Bacete, J., Matsuno-Yagi, A., and Yagi, T. (2010) Pivotal Roles of Three Conserved Carboxyl Residues of the NuoC (30k) Segment in the Structural Integrity of Proton-Translocating NADH-Quinone Oxidoreductase from *Escherichia coli*. *Biochemistry 49*, 10072−10080.

(39) Sinha, S. C., Sinha, S. C., and Keinan, E. (1999) Total Synthesis of Squamotacin. *J. Org. Chem. 64*, 7067−7073.

DOI: 10.1021/bi501403t
Biochemistry 2015, 54, 753−764

(40) Link, A. J., Phillips, D., and Church, G. M. (1997) Methods for generating precise deletions and insertions in the genome of wild-type *Escherichia coli*: application to open reading frame characterization. *J. Bacteriol. 179*, 6228−6237.
(41) Sinha, P. K., Torres-Bacete, J., Nakamaru-Ogiso, E., Castro-Guerrero, N., Matsuno-Yagi, A., and Yagi, T. (2009) Critical roles of subunit NuoH (ND1) in the assembly of peripheral subunits with the membrane domain of *Escherichia coli* NDH-1. *J. Biol. Chem. 284*, 9814−9823.
(42) Ghelli, A., Benelli, B., and Degli Esposti, M. (1997) Measurement of the membrane potential generated by complex I in submitochondrial particles. *J. Biochem. (Tokyo) 121*, 746−755.
(43) Amarneh, B., and Vik, S. B. (2003) Mutagenesis of Subunit N of the *Escherichia coli* Complex I. Identification of the Initiation Codon and the Sensitivity of Mutants to Decylubiquinone. *Biochemistry 42*, 4800−4808.
(44) Torres-Bacete, J., Sinha, P. K., Matsuno-Yagi, A., and Yagi, T. (2011) Structural Contribution of C-terminal Segments of NuoL (ND5) and NuoM (ND4) Subunits of Complex I from *Escherichia coli*. *J. Biol. Chem. 286*, 34007−34014.
(45) Biasini, M., Bienert, S., Waterhouse, A., Arnold, K., Studer, G., Schmidt, T., Kiefer, F., Cassarino, T. G., Bertoni, M., Bordoli, L., and Schwede, T. (2014) SWISS-MODEL: modelling protein tertiary and quaternary structure using evolutionary information. *Nucleic Acids Res. 42*, W252−W258.
(46) Grgic, L., Zwicker, K., Kashani-Poor, N., Kerscher, S., and Brandt, U. (2004) Functional significance of conserved histidines and arginines in the 49 kDa subunit of mitochondrial complex I. *J. Biol. Chem. 279*, 21193−21199.
(47) Belevich, G., Euro, L., Wikstrom, M., and Verkhovskaya, M. (2007) Role of the Conserved Arginine 274 and Histidine 224 and 228 Residues in the NuoCD Subunit of Complex I from *Escherichia coli*. *Biochemistry 46*, 526−533.
(48) Flemming, D., Hellwig, P., and Friedrich, T. (2003) Involvement of tyrosines 114 and 139 of subunit NuoB in the proton pathway around cluster N2 in *Escherichia coli* NADH:ubiquinone oxidoreductase. *J. Biol. Chem. 278*, 3055−3062.
(49) Matsushita, K., Ohnishi, T., and Kaback, H. R. (1987) NADH-ubiquinone oxidoreductases of the *Escherichia coli* aerobic respiratory chain. *Biochemistry 26*, 7732−7737.
(50) Tocilescu, M. A., Fendel, U., Zwicker, K., Drose, S., Kerscher, S., and Brandt, U. (2010) The role of a conserved tyrosine in the 49-kDa subunit of complex I for ubiquinone binding and reduction. *Biochim. Biophys. Acta 1797*, 625−632.
(51) Marin, S. E., Mesterman, R., Robinson, B., Rodenburg, R. J., Smeitink, J., and Tarnopolsky, M. (2013) Leigh Syndrome Associated with Mitochondrial Complex I Deficiency Due to Novel Mutations In NDUFV1 and NDUFS2. *Gene 516*, 162−167.
(52) Murai, M., Sekiguchi, K., Nishioka, T., and Miyoshi, H. (2009) Characterization of the Inhibitor Binding Site in Mitochondrial NADH-Ubiquinone Oxidoreductase by Photoaffinity Labeling Using a Quinazoline-Type Inhibitor (dagger). *Biochemistry 48*, 688−698.
(53) Nakanishi, S., Abe, M., Yamamoto, S., Murai, M., and Miyoshi, H. (2011) Bis-THF motif of acetogenin binds to the third matrix-side loop of ND1 subunit in mitochondrial NADH-ubiquinone oxidoreductase. *Biochim. Biophys. Acta 1807*, 1170−1176.
(54) Satoh, T., Miyoshi, H., Sakamoto, K., and Iwamura, H. (1996) Comparison of the inhibitory action of synthetic capsaicin analogues with various NADH-ubiquinone oxidoreductases. *Biochim. Biophys. Acta 1273*, 21−30.
(55) Nakamaru-Ogiso, E., Han, H., Matsuno-Yagi, A., Keinan, E., Sinha, S. C., Yagi, T., and Ohnishi, T. (2010) The ND2 subunit was labeled by a photoaffinity analogue of asimicin, a potent complex I inhibitor. *FEBS Lett. 584*, 883−888.
(56) Murai, M., and Miyoshi, H. (2014) Chemical modifications of respiratory complex I for structural and functional studies. *J. Bioenerg. Biomembr. 46*, 313−321.
(57) Sazanov, L. A. (2014) The mechanism of coupling between electron transfer and proton translocation in respiratory complex I. *J. Bioenerg. Biomembr. 46*, 247−253.
(58) Rossman, M. G., Moras, D., and Olsen, K. W. (1974) Chemical and biological evolution of a nucleotide-binding protein. *Nature 250*, 194−199.
(59) Darrouzet, E., Issartel, J. P., Lunardi, J., and Dupuis, A. (1998) The 49-kDa subunit of NADH-ubiquinone oxidoreductase (Complex I) is involved in the binding of piericidin and rotenone, two quinone-related inhibitors. *FEBS Lett. 431*, 34−38.
(60) Patsi, J., Maliniemi, P., Pakanen, S., Hinttala, R., Uusimaa, J., Majamaa, K., Nystrom, T., Kervinen, M., and Hassinen, I. E. (2012) LHON/MELAS overlap mutation in ND1 subunit of mitochondrial complex I affects ubiquinone binding as revealed by modeling in *Escherichia coli* NDH-1. *Biochim. Biophys. Acta 1817*, 312−318.
(61) Berrisford, J. M., and Sazanov, L. A. (2009) Structural basis for the mechanism of respiratory complex I. *J. Biol. Chem. 284*, 29773−29783.
(62) Larkin, M. A., Blackshields, G., Brown, N. P., Chenna, R., McGettigan, P. A., McWilliam, H., Valentin, F., Wallace, I. M., Wilm, A., Lopez, R., Thompson, J. D., Gibson, T. J., and Higgins, D. G. (2007) Clustal W and Clustal X version 2.0. *Bioinformatics 23*, 2947−2948.
(63) DeLano, W. L. (2008) *The PyMOL Molecular Graphics System*, DeLano Scientific LLC, Palo Alto, CA, USA, http://www.pymol.org.

DOI: 10.1021/bi501403t
Biochemistry 2015, 54, 753−764